Influences of Etchants on Etched Surfaces of High-Strength and High Conductivity Cu Alloy of Different Processing States

Jinyang Fang , Qingke Zhang * , Xinli Zhang , Feng Liu , Chaofeng Li , Lijing Yang , Cheng Xu , Zhenlun Song

Posted Date: 1 April 2024

doi: 10.20944/preprints202404.0019.v1

Keywords: Cu alloy; Etching; Ferric chloride; Copper chloride; Surface morphology; Roughness

Article

Influences of Etchants on Etched Surfaces of High-Strength and High Conductivity Cu Alloy of Different Processing States

Jinyang Fang [1,2], Qingke Zhang [2,*], Xinli Zhang [3], Feng Liu [4], Chaofeng Li [3], Lijing Yang [2], Cheng Xu [2] and Zhenlun Song [2]

[1] School of Materials Science and Engineering, Jiangxi University of Science and Technology, Ganzhou, 341000, China; fangjinyang@nimte.ac.cn
[2] Key Laboratory of Marine Materials and Related Technologies, Zhejiang Key Laboratory of Marine Materials and Protective Technologies, Ningbo Institute of Materials Technology and Engineering, Chinese Academy of Sciences, Ningbo, 315201, China; yanglj@nimte.ac.cn (L.Y.); xucheng@nimte.ac.cn (C.X.); songzhenlun@nimte.ac.cn (Z.S.)
[3] Ningbo Kangqiang Electronics Co., Ltd., Ningbo 315105, China; zhangxl@kangqiang.com (X.Z.); lcf@kangqiang.com (C.L.)
[4] Ningbo Xingye Shengtai Group Co., Ltd., Ningbo 315336, China; liuf@cn-shine.com
* Correspondence: zhangqingke@nimte.ac.cn; Tel.: +86-574-8668-5893

Abstract: With continuous increase in integration of the semiconductor devices, the requirements on size accuracy and surface quality of the etched lead frame are higher. The etchant is a key factor on etching process and etched surface quality, while effects of the difference in etchants on microscopic etched surface morphology of the Cu alloy have not been directly studied. In this study, the aqua regia, acidic $FeCl_3$ and $CuCl_2$ solutions were used as etchants, and different CuCrSn specimens were etched and characterized. The results show that the etching rate in aqua regia is high, and the grain orientation, grain boundary (GB) and dislocation have significant influence on the local etching rate. The preferential etching of some atomic planes forms steps between grains with different orientations, and the preferential etching around the GB and dislocation group forms grooves, resulting in high surface roughness. For the surfaces etched by the $FeCl_3$ and $CuCl_2$ etchants, the steps and grooves are blurred, thus their roughnesses are much lower. The CuCrSn alloy surface etched by the aqua regia is clean, with little Cr-rich particles, while high density Cr-rich particles are remained on the surfaces etched with the $FeCl_3$ and $CuCl_2$ etchants. For the same kind of etchant, the ion concentration can affect the etching mechanism and etching surface morphology.

Keywords: Cu alloy; etching; ferric chloride; copper chloride; surface morphology; roughness

1. Introduction

The lead frames are widely used for electrical connection between chips and the external circuit in semiconductor packaging. With the development of semiconductor devices towards higher integration, the requirements on size accuracy and surface quality of the lead frames are more and more strict [1]. At present, the high-precision lead frame is mainly processed by etching [2,3], and the materials are the high-strength and high conductivity Cu alloys [4,5]. Etching is a precise material reduction processing method which selectively dissolves the unnecessary part of the Cu alloy strips to obtain the devices with specific size and shape. Therefore, both the etchant and microstructure of the Cu alloy will affect the etching chemical reaction and the etched surface.

The Cu alloy foil can be processed by a variety of etchants with different etching characteristics [6]. Among these etchants, the acidic $FeCl_3$ solution is a common etchant composed mainly of ferric chloride and strong acids, which has fast etching rate and suitable for small-scale etching process of

 doi:10.20944/preprints202404.0019.v1

Cu [7–10]. Compared with the $FeCl_3$ etchant, the acidic $CuCl_2$ etchant has slower etching rate, while the Cu dissolve capacity of the acidic $CuCl_2$ etchant is higher than that of the $FeCl_3$ etchant, thus it is suitable for large-scale etching of Cu [11–14]. Besides, the alkaline $CuCl_2$ etchant composed of ammonia, ammonium chloride and $CuCl_2$ is also widely used in the etching of Cu foils [12,15], but it can change the chemical properties of the resist mask on the lead frame and making it difficult to remove [16]. In addition, some strong acids such as the nitric acid, sulfuric acid or the aqua regia can also etch the Cu alloy [17–19]. Recently, the influences of microstructure and defects on etching behaviors, etched surface morphology and roughness of the Cu alloy etched by aqua regia have been revealed [20,21]. Whereas, to obtain precise etching lead frame with high size accuracy and proper surface roughness, it is necessary to further understand the etching characteristics of the Cu alloy in different etchants, and effects of the microstructure of the Cu alloy on the etching behaviors in different etchants has not yet been directly investigated.

For the reasons above, in this study the aqua regia, acidic $FeCl_3$ and two acidic $CuCl_2$ were selected as the etchants. The aqua regia is a typical strong acid etchant similar to the H_2SO_4-H_2O_2 and the HNO_3 etchant, which can obtain clean etched surface that can be easily observed, thus it is selected to compare with the widely used acidic $FeCl_3$ and acidic $CuCl_2$ etchants. The CuCrSn alloy was selected to be the experimental material based on some earlier investigations, which is a new CuCr series high-strength and high-conductive [22,23]. The CuCrSn alloy specimens of different processing states were firstly etched using the above etchants, then the etched surface morphologies observed and the surface roughness were measured. Based on that, the etching behaviors of the CuCrSn alloy in the different etchants and influences of the microstructure of the Cu alloy on the etched surface were discussed. It is expected that this work can provide a reference for controlling the etching accuracy and etched surface of the lead frame.

2. Materials and Methods

2.1. Preparation of Materials

In this study, the CuCrSn specimen used was smelted in an atmosphere protection furnace with Ar of 99.99% purity as the shielding gas. The raw materials are pure Cu (99.99 wt%), Cu-10Cr intermediate alloy and the Sn particles with purity of 99.99wt%. The designed composition of the alloy is Cu-0.45Cr-0.25Sn (wt%), and the raw materials were weighed according to such a composition. To decrease the burning loss during the smelting process, the internal temperature of the furnace was first heated to 1000 °C, and then the raw materials were put into the graphite crucible. The furnace was continue heated to 1250 °C and kept for 50 min. After that, the liquid alloy was casted in a mold and air cooled to obtain ingots of 10 mm in thickness.

To make the composition more uniform, the CuCrSn cast ingot was homogenized annealed at 960 °C for 6 h, and then cooled with the furnace. The composition of the ingot was analyzed by an inductively coupled plasma emission spectrometry (ICP-OES, Spectro AcroII), and the results show that the mass fractions of the Sn and Cr elements in the alloy were 0.253% and 0.437%, respectively, which were quite close to the designed contents. The homogenized CuCrSn alloy specimen was cold-rolled to 2 mm, and thus the cold rolling deformation is 80%. To obtain CuCrSn specimens with different microstructure and grain size, the cold-rolled specimens were annealed at 600 °C, 700 °C, 750 °C, 800 °C and 850 °C for 15 min.

2.2. Etching and Characterization Methods

The surface microstructure of the cold-rolled and annealed specimens before etching was observed by metallographic microscope (NMM-800RF). For all CuCrSn specimens, the cross sections parallel with the cold rolling direction of the plates were observed. The grinding and polishing processes of all the specimens are as follows: sequentially ground with 500#, 1000#, 1500#, 2000# and 3000# sandpaper, followed by vibrationally polishing with the 2.5 μm and 0.5 μm sized diamond polishing agents. To clearly show the grains of the alloy specimens, the proportion of the corrosion

 doi:10.20944/preprints202404.0019.v1

solution used for the metallographic etching was 5 g ferric chloride hexahydrate +10 ml concentrated hydrochloric acid+100 ml absolute ethanol.

The composition of the acidic $FeCl_3$ etchant is 45 g $FeCl_3 \cdot 6H_2O$+100 ml deionized water+10 ml concentrated hydrochloric acid. Two different $CuCl_2$ etchants were used. The composition of the first is 20 g $CuCl_2 \cdot 2H_2O$+100 ml deionized water+15 ml concentrated hydrochloric ($CuCl_2$-1), and the composition of the second is 28.5 g $CuCl_2 \cdot 2H_2O$+112 ml deionized water+10 ml concentrated hydrochloric acid ($CuCl_2$-2). The contents of the Cu^{2+} and Cl^- in the $CuCl_2$-1 etchant are 1.0 mol/L and 3.24 mol/L, and are 1.3 mol/L and 3.38 mol/L in the $CuCl_2$-2 etchant, respectively. The aqua regia was made by mixing concentrated nitric acid and concentrated hydrochloric acid in the ratio of 1:3, and it was kept for 1 h after mixing so that the two acids can fully react. All the specimens were etched in the etchants for 3 min. The etched surfaces were ultrasonic cleaned and then observed by scanning electron microscope (SEM, FEI Sirion 200) and confocal laser scanning microscope (CLSM, Zeiss LMS700), and the surface roughness was also measured by the CLSM. The distributions of the elements content on the etched surfaces measured by energy dispersive spectrometer (EDS).

3. Results and Discussion

3.1. Grain Structure of Specimens Annealed at Different Temperature

The microstructures of the cold-rolled CuCrSn alloy before and the annealing are shown in Figure 1. Before the annealing, the cold-rolled specimen shows a typical rolling texture structure, and high density deformation defects and grain boundaries (GBs) can be observed, as shown in Figure 1a. The cold-rolling process results in a large number of dislocations and defects, which decreases the binding energy and becomes the preferential etching site [24,25]. Meanwhile, grain fragmentation also occurs, thus the density of GBs increases significantly. After annealed at 600 °C for 15 min, recrystallization occurs in almost all the area, forming very fine grains, and meanwhile the deformation texture has been eliminated (see Figure 1b). As the annealing temperature increases, the grain size increases gradually, while the defects in the Cu alloys are basically not observed, as presented in Figure 1c–f, because the annealing treatment can eliminate most of the dislocations and some other point defects induced during the cold rolling process. As most of the defects have been eliminated, some precipitation particles can be clearly identified in the specimens annealed at higher temperature. Generally, the deformation texture and defects are eliminated and recrystallized grains with different size are obtained after annealing at different temperature.

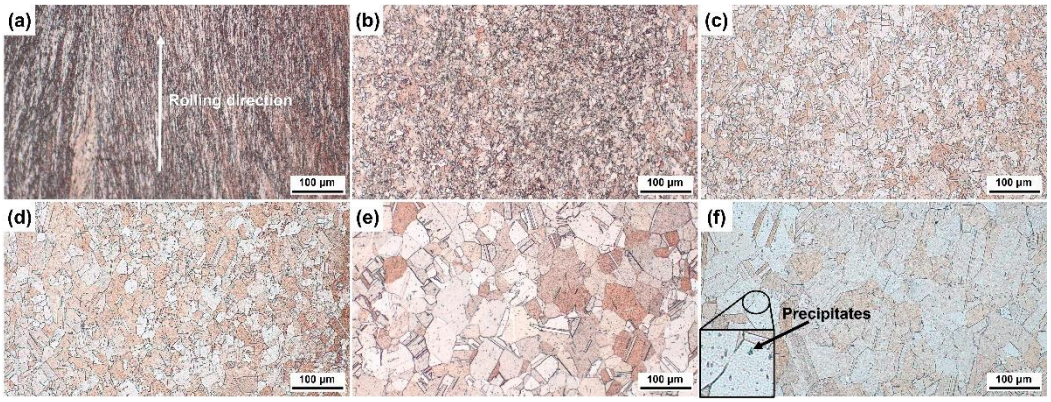

Figure 1. Microstructures of the different CuCrSn specimens: (a) the 80% cold-rolled specimen without annealing, and the specimens further annealed at (b) 600 °C, (c) 700 °C, (d) 750 °C, (e) 800 °C and (f) 850 °C for 15 min after cold-rolling.

3.2. Surface Morphologies after Etching with Different Etchants

Surface morphologies of the different CuCrSn alloy specimens etched for 3 min in the aqua regia etchant are shown in Figure 2. For the 80% cold-rolled specimen, high density etching grooves can be observed on the etched surface, as exhibited in Figure 2a, because dislocation groups and GBs are

 doi:10.20944/preprints202404.0019.v1

formed during the cold-rolling, and the Cu atoms close to these locations are preferentially dissolved. The deep etch grooves will increase the adhesion strength between the molding compound and the etched lead frame. After annealed at 600 °C and 700 °C, the dislocations and the original parallel GBs disappear, and high density new GBs are formed, as shown in Figure 2b,c. Although dissolution of Cu atoms close to the GBs is faster and thus the GBs are etched preferentially, the difference in etching rates between different grains is not very serious, and the etched surface remains relatively flat for the grains are fine. The etched surface morphologies of specimens annealed at higher temperature are shown in Figure 2d–f, in which the grains become larger, and the difference in the etching rates of grains with different orientation gradually emerges. As a result, some protruded grains are formed, because the etching rates of these grains are lower, and some steps are formed at the GBs. Meanwhile, as the density of the GBs decreases, the effect of GBs on the etching becomes less serious. In addition, it has been found by the authors that that the microscopic etched surface morphologies of different grains are very different and basically dominated by the orientation of these grains, and the mechanisms have been revealed [21], thus it will not be deeply analyzed again in this paper.

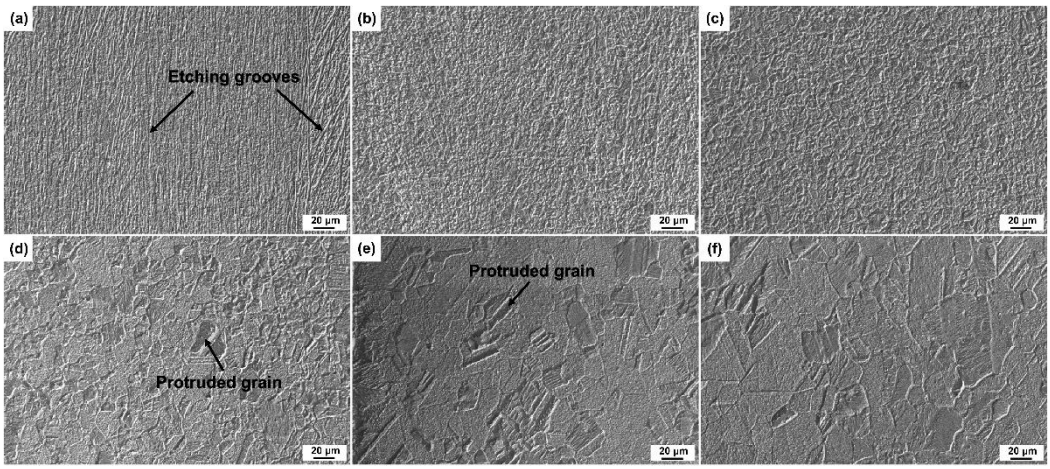

Figure 2. Surface morphologies of the different CuCrSn specimens etched by the aqua regia: (a) the 80% cold-rolled specimen without annealing, and the specimens further annealed at (b) 600 °C, (c) 700 °C, (d) 750 °C, (e) 800 °C and (f) 850 °C for 15 min after cold-rolling.

The surface appearances of the CuCrSn specimens etched for 3 min in the $FeCl_3$ etchant are shown in Figure 3. It can be found that effects of the GBs, grain orientation and dislocation groups on the etching can still be seen. For the cold-rolled specimen shown in Figure 4a, the etching grooves at the GBs and dislocation groups are obvious. Whereas, compared with the specimen surface etched by the aqua regia, the etch grooves at GBs and the dislocation groups become blurred. In Figure 4b,c, although recrystallization has occurred, it is difficult to distinguish the GBs. As the annealing temperature increases, the grain size becomes larger and the difference in etching rate due to different grain orientations becomes more and more obvious. In Figure 4d, clear height difference between the neighboring grains can already be seen, and this difference becomes more obvious in Figure 4e,f. However, the steps at the GBs are not so sharp as that on the surface etched by the aqua regia. In addition, the microstructures of the etched surfaces of different grains are very similar, and some residual particles can be found on the etched surfaces.

 doi:10.20944/preprints202404.0019.v1

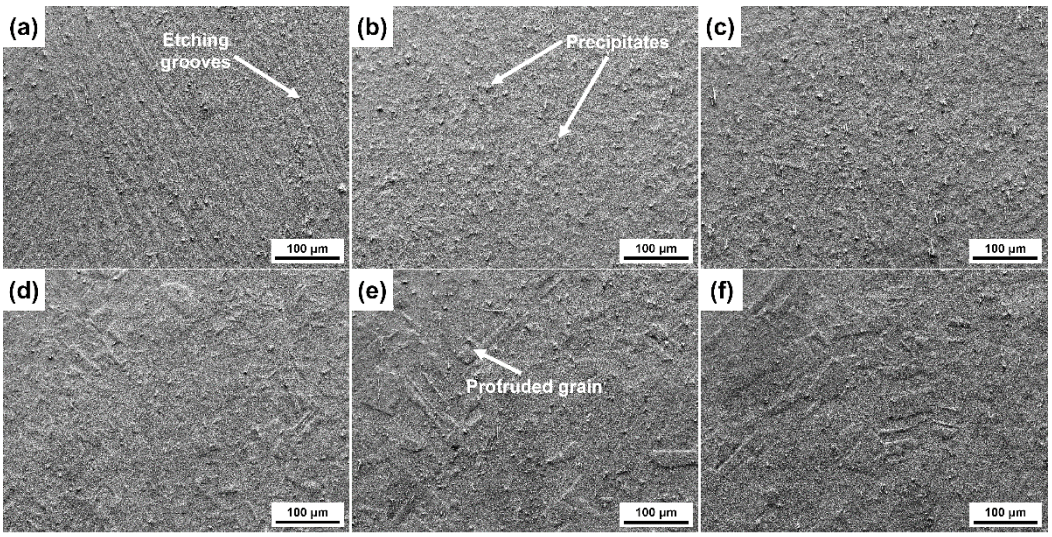

Figure 3. Surface morphologies of the different CuCrSn specimens etched by acidic $FeCl_3$ etchant: (a) the 80% cold-rolled specimen without annealing, and the specimens further annealed at (b) 600 °C, (c) 700 °C, (d) 750 °C, (e) 800 °C and (f) 850 °C for 15 min after cold-rolling.

Figure 4 shows the morphology and composition of the particles on the surface etched by $FeCl_3$ etchant. In Figure 4, it can be found that the size of the bright particles ranges from one to a few micrometers, and have different shapes. The elemental distribution obtained by EDS mapping reveals that these particles are Cr-rich phase precipitates, which was also observed in Figure 1. Figure 5b,c show the EDS point analysis sites and the corresponding composition, which also demonstrates that the particles are Cr-rich phase, and the rest of the surface is almost pure Cu. The presence of these residual particles should be due to the very low dissolution rate of the Cr-rich phase in the $FeCl_3$ etchant. These particles on the surface can hardly be removed by ultrasonic cleaning, thus if they are too large in size, they may be detrimental to the bonding of the molding compound in the subsequent packaging process.

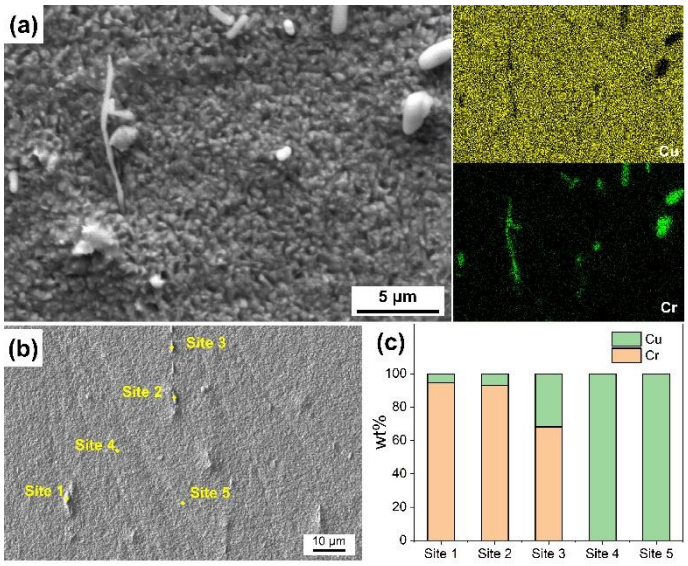

Figure 4. (a) Microscopic surface morphology and elemental distribution of the 80% cold-rolled specimen after etched by the $FeCl_3$ etchant, (b) sites for the EDS characterization and (c) compositions of these sites.

Figure 5 exhibits the surface morphologies of the CuCrSn specimens etched by the $CuCl_2$-1 etchant. As can be seen from Figure 5a, the dislocation groups and a large number of GBs generated by cold-rolling are indistinguishable. With the recrystallization and growth in size of the grains, the

 doi:10.20944/preprints202404.0019.v1

influence of grain orientation on the etched surface morphology is still not obvious, and there is almost no protruded grain on the etched surfaces, as shown in Figure 5b–f. As a result, all the specimens in Figure 5 have very similar morphology after etching. There are also surface residual particles on the etched surface, but their size is smaller than that in Figure 3.

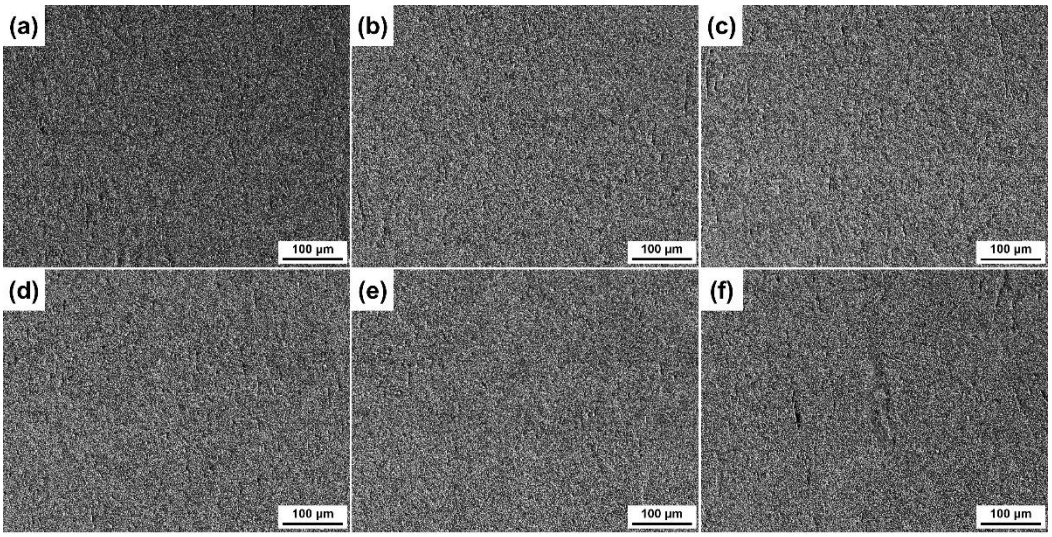

Figure 5. Surface morphologies of the different CuCrSn specimens etched by the $CuCl_2$-1 acidic etchant: (a) the 80% cold-rolled specimen without annealing, and the specimens further annealed at (b) 600 °C, (c) 700 °C, (d) 750 °C, (e) 800 °C and (f) 850 °C for 15 min after cold-rolling.

The surface morphologies of the CuCrSn specimens etched by the $CuCl_2$-2 etchant are presented in Figure 6. For the cold-rolled specimen, the dislocation groups and GBs have little effect on etching, and the surface is flat, as shown in Figure 6a. Whereas, after the recrystallization occurs, effects of the grain orientation on the etching rate become visible, and some slight protrusions can be observed (see Figure 6b–f). Therefore, it can be predicated that even for the same etchant, the concentrations of the ions will affect the etching behavior.

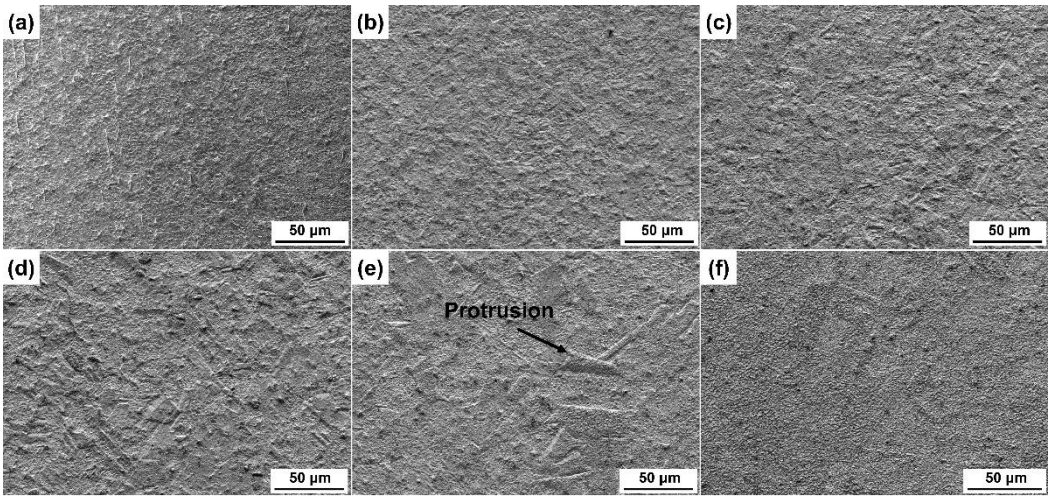

Figure 6. Surface morphologies of the different CuCrSn specimens etched by the $CuCl_2$-2 acidic etchant: (a) the 80% cold-rolled specimen without annealing, and the specimens further annealed at (b) 600 °C, (c) 700 °C, (d) 750 °C, (e) 800 °C and (f) 850 °C for 15 min after cold-rolling.

Figure 7 shows the surface morphologies and elemental distributions on the surfaces etched by the two $CuCl_2$ etchants. For the surface etched by the $CuCl_2$-1 etchant, the surface microstructure is very fine, as shown in Figure 7a. Some residual fine Cr-rich precipitates can be seen on the etched surface. For the surface etched by the $CuCl_2$-2 etchant shown in Figure 7b, it seems that is not so

Preprints.org (www.preprints.org) | NOT PEER-REVIEWED | Posted: 1 April 2024 doi:10.20944/preprints202404.0019.v1

uniform as that of Figure 7a, and the surface roughness is higher. From the microscopic etched surface morphologies, it can be predicted that the ion concentration of the $CuCl_2$ etchant affects the etching process and morphology of the etched surface. With higher concentration of ions, the etching rate will be higher the surface also become coarser.

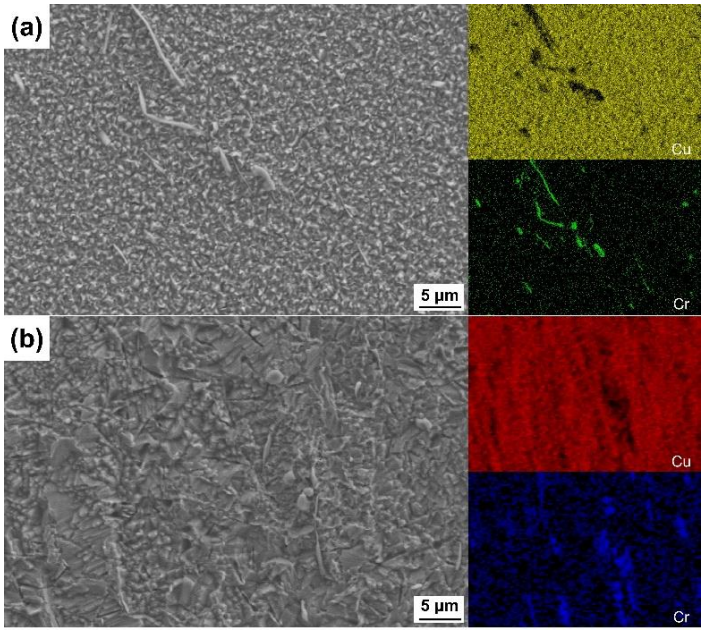

Figure 7. Surface morphologies and elemental distributions of the 80% cold-rolled specimen etched by the: (a) $CuCl_2$-1 and (b) $CuCl_2$-2 etchants.

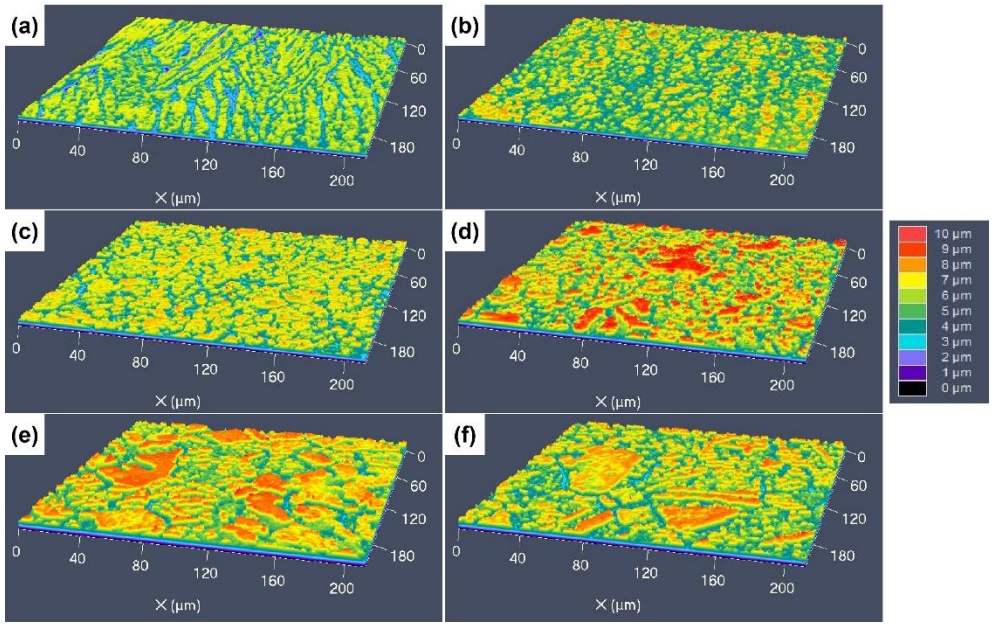

Figure 8. 3D morphologies of the different CuCrSn specimens etched by aqua regia: (a) the 80% cold-rolled specimen without annealing, and the specimens further annealed at (b) 600 °C, (c) 700 °C, (d) 750 °C, (e) 800 °C and (f) 850 °C for 15 min after cold-rolling.

3.3. 3D Surface Undulations after Etching with Different Etchants

The 3D surface morphologies of the specimens etched by the 4 different etchants were characterized using the LSCM, in order to reveal the difference in height between different areas of the etched surfaces, with different colors indicating the difference in height. Figure 9 shows the 3D morphologies of the specimens etched with the aqua regia. For the cold-rolled specimen, the deep

 doi:10.20944/preprints202404.0019.v1

grooves locate at the GBs and dislocation groups can be clearly seen, and the difference in height between the grooves and the surrounding areas is about 3-4 μm. After an annealing at 600 °C, the deepest sites on the etched surface locate at the GBs, as presented in Figure 9b, and the difference in etch rates of different grains is not very obvious. As the annealing temperature increases, some protrusions with red color appear, as shown in Figures 9c-f. The obvious difference in the etching rate occurs not only at the GBs and inside the grains, but also between different grains. Therefore, some red areas can be observed on the etched surfaces, and the height differences on the etched surfaces are about 5-6 μm.

Figure 9 shows the 3D surface morphologies of the specimens etched using the $FeCl_3$ etchant. For the original cold-rolled specimen, it seems that the etch grooves at the dislocation groups become blurred. The depth of the etching grooves is only about 1 μm, which is much shallower than that on the surface etched by the aqua regia, and the width reaches to about 20 μm. In Figure 9b,c, some red protrudent particles can be seen, which are the residual Cr-rich precipitations. The height of these particles raised more than 2 μm. With increasing grain size, the protrudent etch-resistant grains can be observed, as presented in Figure 9d–f, as well, but the height of the protrusions is only about 2-3 μm.

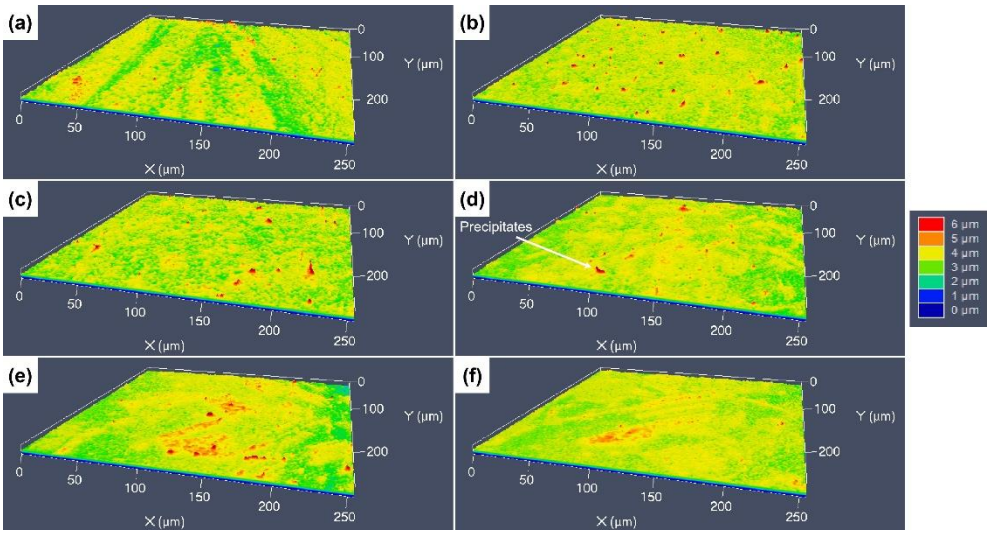

Figure 9. 3D morphologies of the different CuCrSn specimens etched by the $FeCl_3$ etchant: (a) the 80% cold-rolled specimen without annealing, and the specimens further annealed at (b) 600 °C, (c) 700 °C, (d) 750 °C, (e) 800 °C and (f) 850 °C for 15 min after cold-rolling.

The 3D surface morphologies of the specimens etched by the $CuCl_2$-1 etchant are shown Figure 10. It can be found that all the surfaces are very flat, with no obvious protrusion appears, as shown in Figures 10a-c, both the dislocation groups, GBs and grain orientation have little influence on the etching surface. For the specimens with coarser grain, some very fine red particles can still be found on the etched surfaces through careful checking (see Figure 10d–f), which consistent with the SEM images. Figure 11 shows the 3D surface morphology of the specimens etched by the $CuCl_2$-2 etchant, for which the surface fluctuation is higher than that etched by the $CuCl_2$-1 etchant. For the cold-rolled specimen, the deformation defects have little influence on the etching surface, but the grain orientation shows obvious influence and forming some protrudent grains.

Preprints.org (www.preprints.org) | NOT PEER-REVIEWED | Posted: 1 April 2024 doi:10.20944/preprints202404.0019.v1

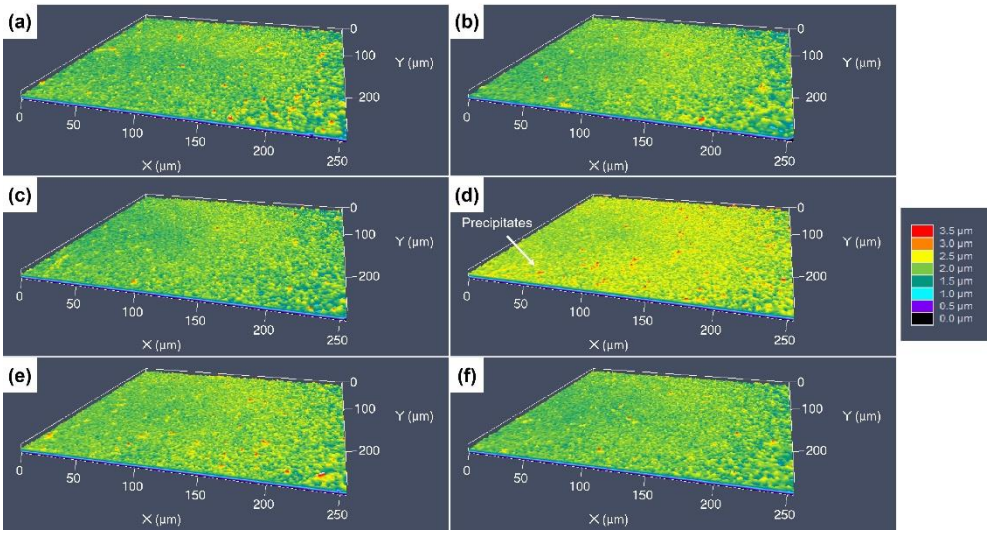

Figure 10. 3D morphologies of the different CuCrSn specimens etched by the $CuCl_2$-1 etchant: (a) the 80% cold-rolled specimen without annealing, and the specimens further annealed at (b) 600 °C, (c) 700 °C, (d) 750 °C, (e) 800 °C and (f) 850 °C for 15 min after cold-rolling.

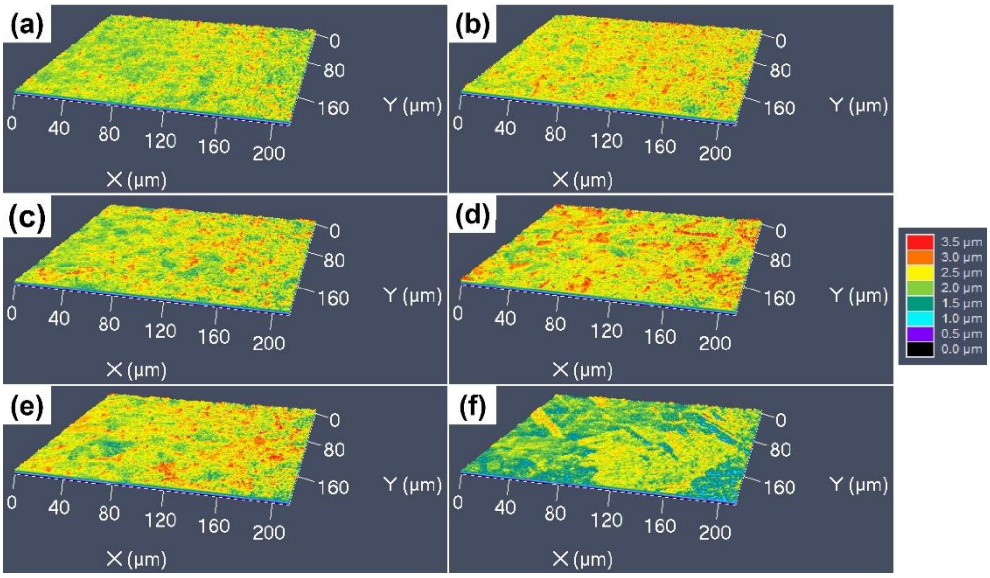

Figure 11. 3D morphologies of the different CuCrSn specimens etched by the $CuCl_2$-2 etchant: (a) the 80% cold-rolled specimen without annealing, and the specimens further annealed at (b) 600 °C, (c) 700 °C, (d) 750 °C, (e) 800 °C and (f) 850 °C for 15 min after cold-rolling.

3.4. Surface Roughness

The obtained surface roughness of the specimens etched by different etchants is shown in Figure 12. For the surfaces etched with aqua regia, the roughness is significantly higher, because the preferential etching at the GBs and dislocation groups in the aqua regia is very serious. Whereas, it seems that the $FeCl_3$ and $CuCl_2$ etchants are insensitive to these defects, thus the GBs and defects are blurred and almost indistinguishable on the etched surface. It has been revealed that the grain size affects the roughness of the CuCrSn alloy surface etched by aqua regia [21]. For the $FeCl_3$ and the two $CuCl_2$ etchants, the recrystallization and grain growth has little influence on the etched surface roughness, although the etched surface morphology is affected by the grain structure, and the annealing temperature (grain size)-surface roughness curves show almost no fluctuation. Figure 13 shows the microscopic surface morphologies of the CuCrSn specimens etched by the 4 etchants, with the same magnification factor, in which the difference in surface roughness is very intuitive.

Preprints.org (www.preprints.org) | NOT PEER-REVIEWED | Posted: 1 April 2024 doi:10.20944/preprints202404.0019.v1

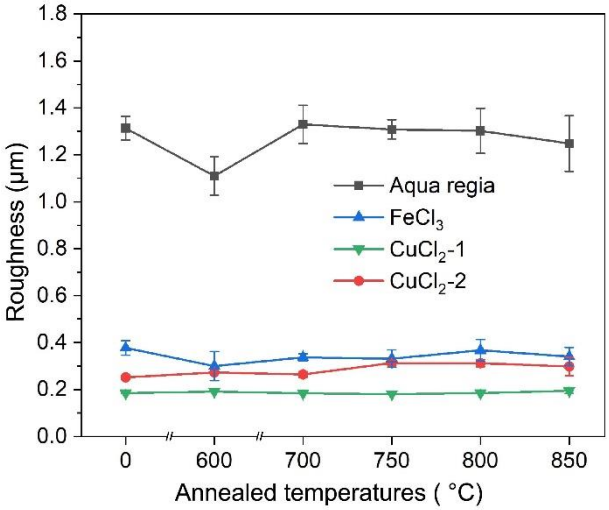

Figure 12. Surface roughness of the CuCrSn alloy specimens etched by the 4 different etchants.

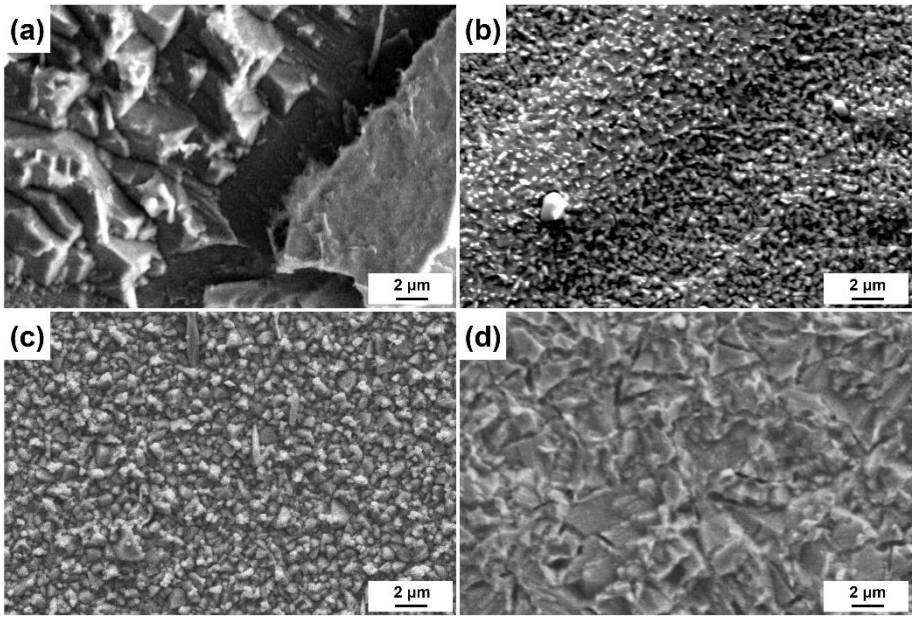

Figure 13. Microscopic surface morphologies of the specimens etched by the: (a) aqua regia, (b) $FeCl_3$, (c) $CuCl_2$-1 and (d) $CuCl_2$-2 etchants.

3.5. Discussion

From the above experimental results, it can be found that the grain structure, GBs and crystal defects of the CuCrSn alloy can affect the etched surface morphology. Whereas, the influence levels of these factors are quite different in the etchants with different etching mechanisms. In the aqua regia, the main substance that reacts with Cu is the concentrated nitric acid and Cl^- is easy to form complexes with Cu^{2+}, which decreases the reduction potential of Cu and accelerates the reaction. The reaction equation is as follows [26]:

$$\mathrm{Cu(s)} + 4\mathrm{H}NO_3(aq) = 2H_2O(l) + 2NO_2(g) + Cu(NO_3)_2(aq) \quad (1)$$

During the etching process, Cu is directly oxidized to Cu^{2+} and then rapidly dissolved. As the reactivity of atoms near the defects and GBs is higher, which accelerates the dissolution rate, the aqua regia etchant is strongly influenced by defects, GBs and crystal orientation. Besides, the bonding energies between different atomic planes are different, resulting in the difference in etching rates of grains with different orientations and step morphologies within the etched surface of the grains.

 doi:10.20944/preprints202404.0019.v1

For the $FeCl_3$ etchant, the Fe^{3+} ion on the surface of alloy oxidize Cu atom to Cu^+, the resulting CuCl is insoluble in the solution and will cover the surface of the alloy. Then, the CuCl can be further oxidized by Fe^{3+} to $CuCl_2$, the reaction equation is as follows [16,27,28]:

$$Cu(s) + FeCl_3(aq) = CuCl(s) + FeCl_2(\text{aq}) \quad (2)$$

$$CuCl(s) + FeCl_3(aq) = CuCl_2(aq) + FeCl_2(aq) \quad (3)$$

For etching in the $FeCl_3$ etchant, the Cu atoms at the surface atoms direct contact with Fe^{3+} at the beginning, thus the etching rate is the fastest. Since the dissolution rate of the CuCl is low than the generation rate, the CuCl film will form on the alloy surface, which prevents the Fe^{3+} from contact with the alloy surface and hinders the reaction (2). As a result, the generation rate of the CuCl film decreases until the generation and dissolution of the CuCl achieve a dynamic equilibrium, and the etching rate begins to stabilize [29,30]. Since there is a CuCl film that affects the etching mechanism, the surface morphology etched with the $FeCl_3$ etchant is obviously different from that etched with the aqua regia. The effects of defects, GBs and grain orientation on etching can still be observed and are suppressed to a high extent.

The reaction processes of the $CuCl_2$ etchant with the Cu alloys are as follows [11–13]:

$$CuCl_2(aq) + Cu(s) = Cu_2Cl_2(s) \quad (4)$$

$$Cu_2Cl_2(s) + 4Cl^- = 2[CuCl_3]^{2-} \quad (5)$$

The Cu^{2+} ion first oxidizes the Cu atom to Cu^+, which also forms the CuCl films. Unlike the $FeCl_3$ etchant, the CuCl film can only be dissolved through the adsorption of Cl^- to form a complex, and the dissolution rate of CuCl film in the $CuCl_2$ etchant is lower than that in the $FeCl_3$ etchant. Figure 14 shows the characterization sites and the corresponding compositions of a specimen etched by the $CuCl_2$-1 etchant, with no ultrasonic cleaning after the etching, which demonstrates that the etched surface before ultrasonic cleaning is almost covered by the CuCl. Therefore, the influence of the CuCl film on the etching process is more serious, while the influence of defects, GBs and grain orientation on the etching process is much weaker, so the consistency of the etched surface in the $CuCl_2$ etchant is better and the surface roughness is much lower. The $CuCl_2$-2 etchant has a higher content of Cl^- and Cu^{2+} than the $CuCl_2$-1 etchant, which is more erosive to the CuCl film, and the etching is less uniform. As the difference in etching rates of $CuCl_2$ to the matrix and the precipitates is low, the residual precipitation particles on the surfaces etched by the $CuCl_2$ etchant are smaller in size.

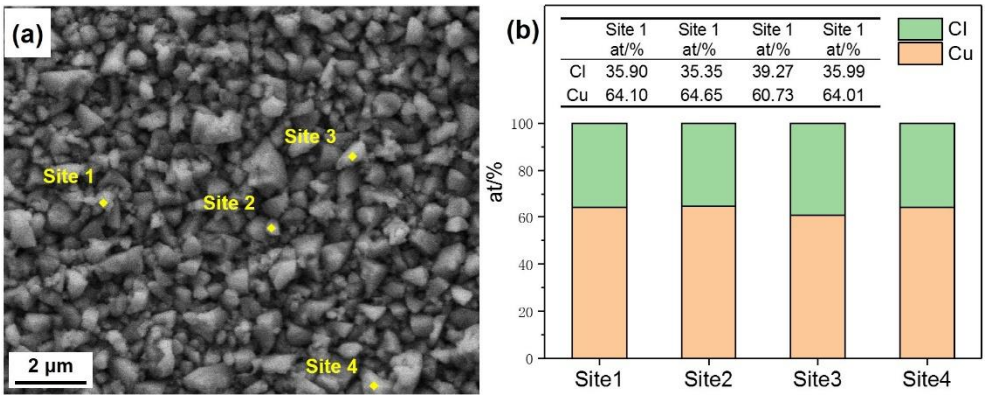

Figure 14. (a) Characterization sites and (b) the corresponding compositions of a specimen etched by the $CuCl_2$-1 etchant, with no ultrasonic cleaning after the etching.

4. Conclusions

The etching surface of a set of the CuCrSn alloy specimens with different microstructure and grain sizes by 4 different etchants (aqua regia, $FeCl_3$, $CuCl_2$-1 and $CuCl_2$-2) were characterized in this study. The main conclusions are as follow:

 doi:10.20944/preprints202404.0019.v1

1. The etching rate in aqua regia is high, and the grain orientation, GBs and dislocations have significant influence on the etching rate. The preferential etching of some atomic planes forms step-like structure between grains with different orientations, and the preferential etching around the GB and dislocation group forms grooves. For etching of the $FeCl_3$ and $CuCl_2$ etchants, such steps and grooves become blurred, and almost invisible on the surface etched by the $CuCl_2$ etchant.

2. The CuCrSn alloy surface etched by the aqua regia is clean, with very little Cr-rich particles. For the specimens etched with the $FeCl_3$ and $CuCl_2$ etchants, high density Cr-rich particles are remained on the surfaces, indicating that etching in these two etchants are more likely to be affected by the alloy composition and the precipitations.

3. Due to the serious difference in etching rate at different locations, the surface roughness of specimen etched by the aqua regia is the highest. There is little fluctuation on the surfaces etched with the $FeCl_3$ and $CuCl_2$ etchants, thus the surface roughness are much lower. For the same kind of etchant, the ion concentration can affect the etching mechanism and etching surface morphology, although not fundamentally.

Author Contributions: Conceptualization, Q.Z. and F.L.; methodology, Q.Z. and J.F.; investigation, J.F.; resources, X.Z. and C.L.; writing—original draft preparation, J.F.; writing—review and editing, Q.Z. and L.Y.; supervision, C.X. and Z.S.; funding acquisition, C.L. and Z.S. All of the authors have read and agreed to the published version of the manuscript.

Funding: This research was funded by the "Scientific and Technological Innovation 2025" Major Special Project of Ningbo City under grant Nos 2021Z049 and 2023Z017.

Institutional Review Board Statement: Not applicable.

Informed Consent Statement: Not applicable.

Data Availability Statement: The data presented in this study are available on request from the corresponding author.

Acknowledgments: The authors would like to acknowledge Y.P. Wei, R.R. Jiang and Y.Y. Yao for the microstructure observation.

Conflicts of Interest: The authors declare that they have no known competing financial interests or personal relationships that could have appeared to influence the work reported in this paper.

References

1. Visser, A.; Buhlert, M. Theoretical and practical aspects of the miniaturization of lead frames by double sided asymmetrical spray etching. J. Mater. Process. Tech. 2001, 115, 108-113.
2. Zhao, W.C.; Feng, R.; Wang, X.W.; Wang, Y.X.; Pan, Y.K.; Gong, B.K.; Han, X.J.; Feng, T.J. Effect of grain boundaries and crystal orientation on etching behavior of 12 μm thick rolled copper foil. Mater. Today. Commun. 2023, 34, 105029.
3. Kim, B.J.; Jeon, H.I.; Kim, G.J.; Cho, N.H.; Khim, J.Y.; Kim, Y.K. Wettable flank routable thin Micro Lead Frame for automotive applications. Microelectron. Reliab. 2022, 135, 114602.
4. Yang, H.Y.; Ma, Z.C.; Lei, C.H.; Meng, L.; Fang, Y.T.; Liu J.B.; Wang, H.T. High strength and high conductivity Cu alloys: A review. Sci. China. Technol. Sc. 2020, 63, 2505-2517.
5. Yang, K.; Wang, Y.H.; Guo, M.X.; Wang, H.; Mo, Y.D.; Dong, X.G.; Lou, H.F. Recent development of advanced precipitation-strengthened Cu alloys with high strength and conductivity: a review. Prog. Mater. Sci. 2023, 138, 101141.
6. Williams, K.R.; Gupta, K.; Wasilik, M. Etch rates for micromachining processing-Part II. J. Microelectromech. S. 2003, 12, 761-778.
7. Çakır, O. Review of etchants for copper and its alloys in wet etching processes. Key. Eng. Mater. 2008, 364, 460-465.
8. Zhang, Y.; Zhang, Z.T.; Yang, J.L.; Yue, Y.K.; Zhang, H.F. Fabrication of superhydrophobic surface on stainless steel by two-step chemical etching. Chem. Phys. Lett. 2022, 797, 139567.
9. Allen, D.M.; Almond H.J.A. Characterization of aqueous ferric chloride etchants used in industrial photochemical machining. J. Mater. Process. Tech. 2004, 149, 238-245,.
10. Çakır, O. Chemical etching of aluminum. J. Mater. Process. Tech. 2008, 199, 337-340.
11. Sheng, J.Z.; Li, H.; Shen, S.N.; Ming, R.J.; Sun, B.; Wang, J.; Zhang, D.D.; Tang, Y.G. Investigation on chemical etching process of FPCB with 18 μm line pitch. IEEE Access 2021, 9, 50872-50879.

 doi:10.20944/preprints202404.0019.v1

12. Çakır, O.; Temel H.; Kiyak, M. Chemical etching of Cu-ETP copper. J. Mater. Process. Tech. 2005, 162, 275-279.
13. Choi, J.C.; Lee, J.H. Etching behaviors of Cu and invar for metal core PCB applications. J. Nanosci. Nanotechno. 2017, 17, 7358-7361.
14. Yang, Z.Y.; Huang, C.D.; Ji, X.Q.; Wang, Y.X. A new electrolytic method for on-site regeneration of acidic copper (II) chloride etchant in printed circuit board production. Int. J. Electrochem. Sc. 2013, 8, 6258-6268.
15. Darchen, A.; Drissi-Daoudi, R.; Irzho, A. Electrochemical investigations of copper etching by Cu (NH3) 4Cl2 in ammoniacal solutions. J. Appl. Electrochem. 1997, 27, 448-454.
16. Wang, S.F.; Ding, F.; Wang, F.W.; Wang, X.; Zou, H.L. Study on reducing side etching of Copper microelectrode by multi-step etching process. Mater. Res. Express. 2019, 6, 126411.
17. Kondo, K.; Kurihara, H.; Murakami, H. Etching morphology of single-crystal copper. Electrochem. Solid. St. 2005, 9, C36.
18. Köllensperger, P.A.; Karl, W.J.; Ahmad, M.M.; Pike, W.T.; Green, M. Patterning of platinum (Pt) thin films by chemical wet etching in Aqua Regia. J. Micromech. Microeng. 2012, 22, 067001.
19. Seo, B.H.; Lee, S.H.; Park, I.S.; Seo, J.H.; Choe, H.H.; Jeon, JH.; Hong, M.P. Effect of nitric acid on wet etching behavior of Cu/Mo for TFT application. Curr. Appl. Phys. 2011, 11, S262-S265.
20. Ralston, K.D.; Birbilis, N. Effect of grain size on corrosion: a review. Corrosion 2010, 66, 075005.
21. Fang, J.Y.; Li, C.F.; Liu, F.; Hou, H.L.; Zhang, X.L.; Zhang, Q.K.; Yang, L.J.; Xu, C.; Song, Z.L. Effects of grain orientation and grain size on etching behaviors of high-strength and high-conductivity Cu alloy. Mater. Today. Commun. 2024, 38, 108111.
22. Peng, L.J.; Xie, H.F.; Huang, G.J.; Xu, G.L.; Yin, X.Q.; Feng, X.; Mi, X.J.; Yang, Z. The phase transformation and strengthening of a Cu-0.71 wt% Cr alloy. J. Alloy. Compd. 2017 708, 1096-1102.
23. Li, J.Z.; Ding, H.; Li, B.M.; Gao, W.L.; Bai, J.; Sha, G. Effect of Cr and Sn additions on microstructure, mechanical-electrical properties and softening resistance of Cu-Cr-Sn alloy, Mater. Sci. Eng. A. 2021, 802, 140628.
24. Yamashita, M.; Mimaki, T.; Hashimoto, S.; Miura, S. Intergranular corrosion of copper and α-Cu-Al alloy bicrystals. Philos. Mag. A 1991, 63, 695-705.
25. Miyamoto, H.; Yoshimura, K.; Mimaki, T.; Yamashita, M. Behavior of intergranular corrosion of< 011> tilt grain boundaries of pure copper bicrystals. Corros. Sci. 2002, 44, 1835-1846.
26. Carlson, R.K.; Yang, P.; Clegg, S.M.; Batista, E.R. Mechanistic Study of the Production of NO x Gases from the Reaction of Copper with Nitric Acid. Inorg. Chem. 2020, 59, 16833-16842.
27. Atta, R.M. Effect of applying air pressure during wet etching of micro copper PCB tracks with ferric chloride. Int. J. Mater. Res. 2022, 113, 795-808.
28. Choi, J.C.; Lee, Y.S.; Lee, J.; Kwon, H.W.; Lee, J.H. Etching behaviors of galvanic coupled metals in PCB applications. In 2018 Pan Pacific Microelectronics Symposium (Pan Pacific). IEEE, Big Island, USA , 05-08 February 2018; pp. 1-4.
29. Jian, C.; Jusheng, M.; Gangqiang, W.; Xiangyun, T. Effects on etching rates of copper in ferric chloride solutions. In 2nd 1998 IEMT/IMC Symposium (IEEE Cat. No. 98EX225). IEEE, Tokyo, Japan, 15-17 August 2002; pp. 144-148.
30. Braun, M.; Nobe, K. Electrodissolution kinetics of copper in acidic chloride solutions. J. Electrochem. Soc. 1979, 126, 1666.